

## Dynamics and stability of supergiant atmospheres

### ABSTRACT

Pressure- and gravity waves are the motion forms possible in a non-magnetic atmosphere. They can be studied by means of a diagnostic diagram, but the effects of the observational micro- and macro-turbulent filters have to be considered. Comparison with observational data shows that in supergiants gravity waves have periods close to the Brunt-Väisälä period, velocity amplitudes about twice that of sound, and wavelengths of the same order as the stellar radius. The pressure waves rapidly transform into shock waves, with typical average wavelengths of about 2.5 times the density scale height  $H$ . In super- and hypergiants they have shock strengths up to about 6 for the most luminous stars. They are associated with a non-zero mass flux and may be the cause of the stellar mass loss. Gravity waves seem to be the cause of atmospheric instability in super- and hypergiants.

### OBSERVATIONAL DATA RELEVANT TO ATMOSPHERIC MOTIONS

Motions in stellar atmospheres can be studied only in a limited number of ways. There are two classical spectroscopic techniques. The first is the study of the small-scale motion field (with characteristic lengths shorter than the mean free path of the photon). This affects the line width and equivalent width, and is called 'microturbulence'. The other is the study of the large-scale motion field (length scale larger than the mean free path of photon), which affects the line profile, not the equivalent width; this is 'macroturbulence'. Observations yield the z-components,  $\zeta_\mu$  and  $\zeta_M$ .

Techniques have been developed to study the depth dependence of  $\zeta_\mu$ ; for the latest developments in this direction see Achmad (1991). By introducing the notion 'mechanical flux'

$$F_m = \alpha \rho (\zeta_\mu)^2 s \quad (1)$$

it is then possible to determine the 'dissipation factor' of mechanical energy

$$f = H d \ln F_m / dz. \quad (2)$$

High-resolution spectral observations sometimes allow one to determine the distribution function of the large scale motion field.

Micro- and macro-turbulence were in the past sometimes called 'fudge-factors', but this is no longer the case, since the physics of the small- and large scale motion fields in supergiants is presently well understood.

A new and promising technique to study atmospheric motions in supergiants is that of astroseismology. But so far only little relevant observational data is available and we have to await future developments.

### MICROTURBULENCE = PRESSURE WAVES; MACRO-TURBULENCE = GRAVITY WAVES

The various kinds of motions that are possible in a non-magnetic atmosphere are governed by the dispersion relation (Hines, 1960):

$$(\omega^2 - \omega_{ac}^2) \omega^2 / s^2 - (\omega/k)^2 + \omega_{BV}^2 k^2 \sin^2 \theta = 0 \quad (3)$$

where  $\omega = 2 \pi / P$  and  $P$  = the period of the waves. Further,  $k = 2 \pi / L$ , with  $L$  = wavelength.  $\theta$  is the angle of propagation, with respect to the z-axis. The two constants in eq. (1) are the acoustic cut-off frequency

$$\omega_{ac} = s/2H, \quad (4)$$

and the Brunt-Väisälä frequency

$$\omega_{BV} = (\gamma - 1)^{0.5} g/s \quad (5)$$

where  $g$  is the effective acceleration of gravity, and  $s$  the velocity of sound.

By solving  $\omega$  as a function of  $k$  and plotting  $\omega$  against  $k$  one obtains a 'diagnostic diagram' which shows the areas where waves are possible and the areas where they are evanescent (for imaginary  $\omega$ ).

Our experience has shown that it is suitable to plot the wave period  $P$  against the wavelength  $L$  (cf. De Jager et al., 1991). Fig. 1 shows such a diagnostic diagram, for a level in the atmosphere of Alpha Per, a Ib supergiant. Gravity waves are possible, in principle, in the area with wavelengths exceeding

those of the line labeled Grav, but only as long as the wave period is smaller than the radiative damping time (curve labeled Trad). The dashed line in the Figure is the Tdamp line, calculated for a homogeneous atmosphere, but layer curvature causes

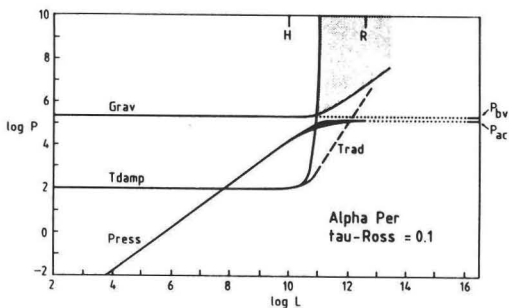


Figure 1: Diagnostic diagram of motions that are possible in the atmosphere of Alpha Per at  $\tau_R = 0.1$

a cut-off at shorter wavelengths - see the full-drawn line. (De Jager et al., 1991). Thus, gravity waves are only possible in a small area with very long  $P$  and  $L$  values. In the case of Alpha Per the possible wavelengths of gravity waves are of the order of the stellar radius, and the periods are  $L.s$ , hence at least of the order of days. Note also that the Grav-line proper corresponds with gravity waves propagating horizontally. Waves with other directions of propagation have longer periods.

The other possible wave mode is the pressure (or: acoustic) waves. They are only possible at the line labeled Press in Fig. 1, including the thickening of the line in its curved part.

In the area where the wave period exceeds the radiative damping time the waves are isothermal, in the other part of the diagram they are adiabatic. It is as a rule assumed that no pressure waves are possible with wavelengths greatly exceeding the 'thickness' of the atmosphere, say of a few scale heights  $H$ . It has been found (De Jager et al., 1991) that the longest waves that occur in the atmospheres of a number of well-studied super- and hypergiants have lengths of about  $4H$ .

In view of the wavelengths involved the pressure waves should mainly be identified with the microturbulent motion component and the gravity waves with the macroturbulent one, but spectroscopic diagnostics sets some further limits, because pressure waves with very long wavelengths may rather broaden the lines in the macroturbulent fashion, while reversely

gravity waves with short wavelengths may contribute to the microturbulence (increasing line broadening as well as the equivalent widths). The question, which parts of the velocity spectrum contribute to either of the two mechanisms or affects both of them (the

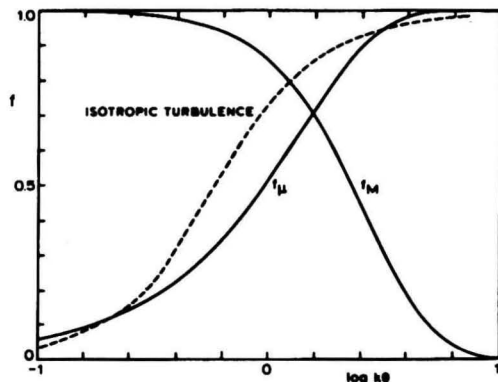


Figure 2: Micro- and macro-turbulent filter functions give for any wavenumber  $k$  the fractions of the motion energy that contributes to the observed micro- or macro- turbulent line broadenings.  $\theta$  is the 'optical scale height' (De Jager and Vermue, 1979). The dashed line was derived by Durrant (1979).

socalled case of mesoturbulence), is answered by deriving the micro- and macro-turbulent filters. These show which fraction of the line of sight energy of the wave motions of a chosen wavenumber  $k$  contributes to the micro- or macroturbulent line broadening (Figure 2). In that Figure  $\theta$  is the 'optical scale height' being the vertical distance over which the optical depth increases by a factor 10, and  $k$  is the wavenumber. The microturbulent filter is for our discussion the most relevant one, because it refers to small-scale upward motions; hence to the pressure wave component. When interpreting data on microturbulence one should be aware of the fact that not all pressure wave energy will in all cases be measured as microturbulence.

### GRAVITY WAVES IN SUPER- AND HYPERGIANTS

Burki (1978) has shown that practically all super- and hypergiants show some sign of variability; a 'quasi period'  $P_q$ , can be defined, where  $P_q$  is actually the most important component in a Fourier analysis of variations of light and/or radial velocity. (Fig. 3).

When comparing the  $P_q$  values with diagnostic

diagrams for the motion fields in supergiants, as done in Figure 4, it appears that  $P_q$  is often the shortest possible period. Hence, the gravity waves that are possible can be found in the lower left corner of the area where gravity waves are theoretically still possible. The periods appear to be close to the Brunt-

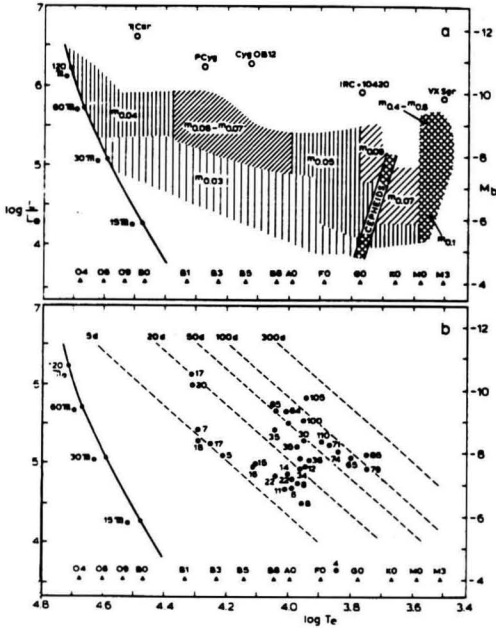


Figure 3: Upper: peak-to-peak values of the V brightness of stars. Lower: approximate lines of constant  $P_q$  values (Burki, 1978)

Väisälä period. This means that the atmospheres oscillate in the highest possible modes. Yet, the mode numbers are fairly small, the wavelengths long. It also means that the gravity waves virtually propagate horizontally, because the line labeled 'Grav' in the diagnostic diagrams corresponds to waves propagating horizontally. For other directions the lines would be situated at longer periods.

Only in cases when very high resolution spectra are available it is possible to become more specific with respect to the large scale motion field. For Alpha Cyg (A2 Ia) it appeared possible (Boer et al., 1988) to deconvolve well-observed, spectrally isolated lines, and thus to eliminate all other broadening effects, in such a way, that the large-scale motion field results (Figure 5). It is bimodal, with average up- and downward velocities of about  $14 \text{ km s}^{-1}$ , which is 1.5 times the velocity of sound. They are in-

terpreted as up- and downward motions of 'elements' with average diameters of  $0.3 R_*$  and average periods of 10 days. At any time there should be 30 to 40 such 'elements' on the visible surface of the star.

From the material so far available it is concluded that on the average the velocity amplitude in super-

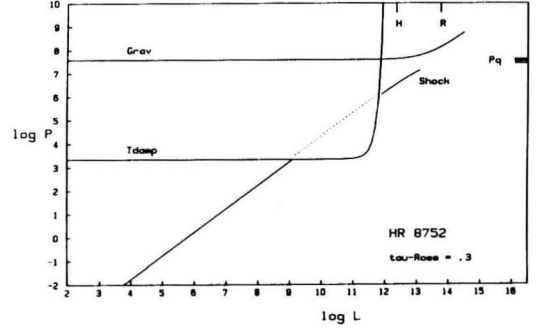


Figure 4: Diagnostic diagram for the atmosphere of HR 8752 (HD 217476, G0-5 Ia+) at  $\tau_R = 0.3$ . Ticks labeled  $P_q$  along the right-hand ordinate refer to various determinations of the quasi-period. If  $P_q$  is identified with gravity waves, the conclusion is that gravity waves originate at the shortest possible wavelengths and periods, close to the Brunt- Väisälä period. In this star the wavelengths corresponding to  $P_q$  are about 20 million km.

and hypergiants is about twice that of sound (De Jager et al., 1991).

We are awaiting the era of astro-seismological research for obtaining more specific information on the large scale motion fields in supergiants.

## MICROTURBULENCE = SHOCK WAVES

Any field of pressure waves will rapidly, typically within one wave period, develop into a field of shock waves, irrespective of whether the waves are isothermal or adiabatic. This is so because in any case the compressed parts of the waves move with higher speed than the expanded parts, causing the waves to assume a saw-tooth velocity profile. A shock-wave (Fig. 6) moves with velocity  $U$ . For an outside observer gas in front of the shock streams towards it with velocity  $v_1$ ; that in the back of the shock has instreaming velocity  $v_2$ . This causes a periodic motion. For an observer moving with the shock matter streams in with  $(U-v_1)$  and out with  $(U-v_2)$ . The latter is smaller than the former, which is related to the fact that the gas is more compressed behind the

shock than in front of it.

The parameter characterizing shocks is the Mach number  $M = (U-v_1)/s_1$  where  $s$  is the velocity of sound. It appears that  $M$  has values close to unity

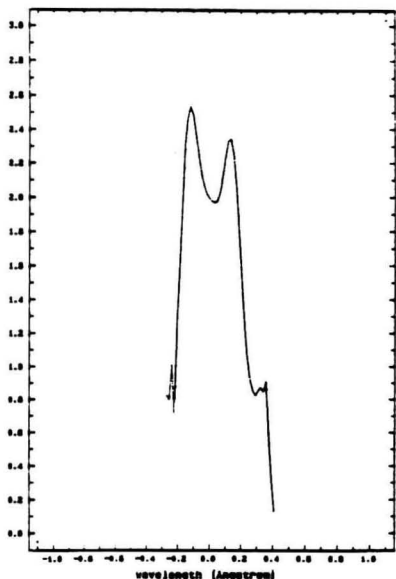


Figure 5: Distribution function of the large-scale motions in Alpha Cyg, after Boer et al. (1988).

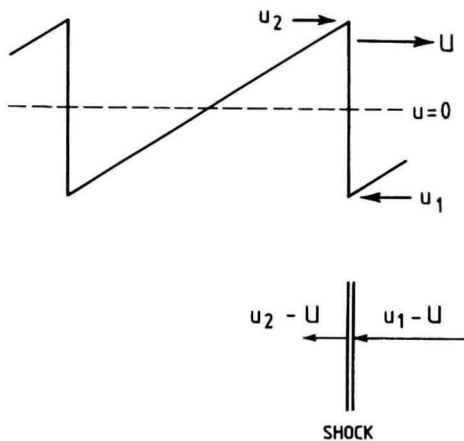


Figure 6: Velocities in shock waves.

for normal giants and moderate supergiants, but its value increases dramatically with luminosity to reach values around 6 for the most luminous supergiants (Nieuwenhuijzen and De Jager, These Proceedings).

When the average microturbulent velocity  $\zeta_\mu$ , the dissipation factor  $f$  of the shock wave mechanical flux, and the shape of the microturbulent filter function are known, further analysis is possible leading to information on the spectral distribution of shock-wave energy. Assuming that the shock wave spectrum has a longest wavelength  $L_0$  (at which wavelength energy is fed into the motion field), assuming further that for shorter wavelengths the spectrum is a power spectrum with exponent  $n$ , then the following expression describes the motion energy at a wavelength  $L$  (De Jager et al., 1991):

$$\zeta^2(L)/\zeta_\mu^2 = (n-1)(L-L_0)^{n-1} \quad (6)$$

For the dissipation factor  $f$  one has (Hearn, 1974)

$$f = 16/3 \cdot (H/L) \cdot (\zeta(L)/s) \quad (7)$$

while the average wavelength is:

$$\langle L \rangle = L_0 n / (n+1) \quad (8)$$

When  $\zeta_\mu$  and  $f$  are known  $L_0$  and  $\langle L \rangle$  can be derived when a value for  $n$  is assumed. The best choice for  $n$  seems  $n = 5/3$ , which applies to a Kolmogoroff spectrum of motion energy. Then  $\langle L \rangle / L_0 = 5/8$ .

For a number of well-studied super- and hypergiants De Jager et al. (1991) have derived values for  $\langle L \rangle$  and  $L_0$ ; it appears that  $L_0$  is of the order of  $4H$ , where  $H$  is the density scale height of the atmosphere. Further,  $\langle L \rangle$  is of the order of  $2.5H$ , with some scatter from one star to another. It may seem surprising that such large values for the average wavelength of the shocks (actually the average vertical distance between successive shocks) are found. This may be due to 'shock cannibalism', an effect described by Cuntz (These Proceedings): since strong shocks move more rapidly than weak ones they tend to sweep up the weaker shocks, resulting in increased shock strengths and wavelengths.

For weak shocks the velocity profile between the shocks can fairly well be described by a linear sawtooth profile, but in stronger shocks the profile becomes more and more convex (De Jager, These Proceedings); see also Figure 7.

This can give rise to a non-zero mass flux; and it seems that the rate of mass loss of giants and supergiants can well be explained by being initiated by

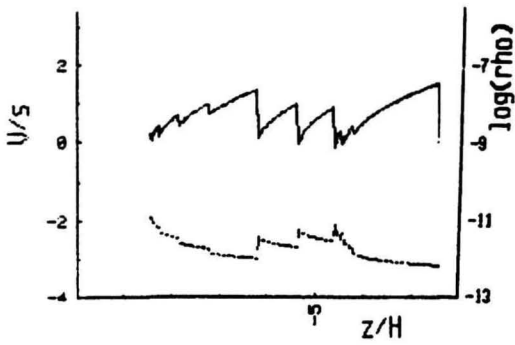


Figure 7: Velocity profile in a strong shock. Upper curve (left ordinate): velocity. Lower curve (right ordinate): density.

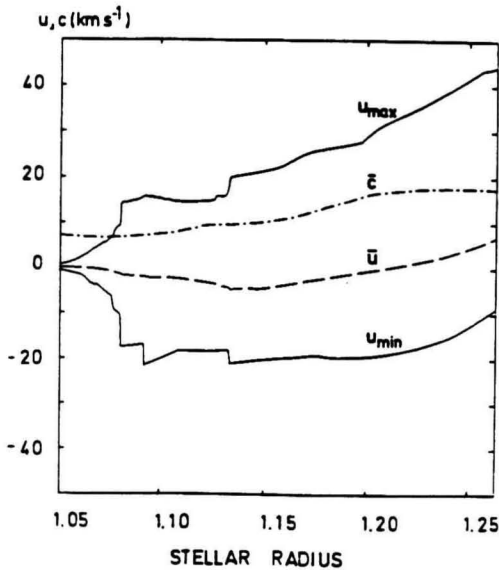


Figure 8: Mass motions in the outer atmosphere of Arcturus after Cuntz (1990). In this diagram  $c$  is the velocity of sound;  $u$  the mass velocity, while also the maximum and minimum values of  $u$  are shown.

shock waves. See also Bowen's paper in These Proceedings. Cuntz (1990) has made some numerical calculations of shock waves in a moderate giant (Arcturus) and found that the average outward velocity

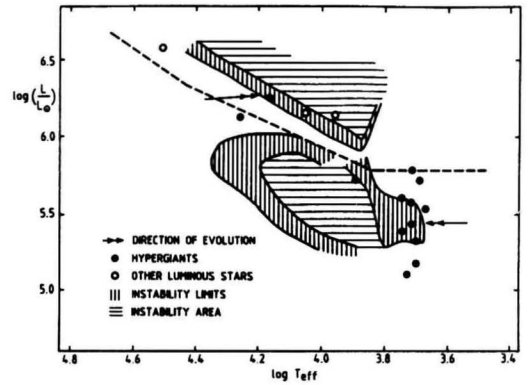


Figure 9: Regions of atmospheric instability in the HR diagram (Nieuwenhuijzen and De Jager, These Proceedings).

component tends to increase with distance from the star (Fig 8).

### STELLAR ATMOSPHERIC STABILITY

Motions are the basic phenomenon for establishing stellar atmospheric instability. The various accelerations working on a unit volume of gas in a stellar atmosphere are described by Nieuwenhuijzen and De Jager (These Proceedings). One has to distinguish between 'constant' accelerations (meaning those that only change on a time scale long as compared with the dynamical time scale of the atmosphere, which is of the order of  $H/s$ ), and time dependent ones, typically the gravity waves.

The 'constant' accelerations are those due to gravity (downward = negative), radiation (positive), shock wave pressure (positive), shock wave momentum transfer (positive) and to the stellar wind reaction force (negative). The first and the last mentioned stabilize the atmosphere, the others destabilize. When the sum of all accelerations is negative, the relevant part of the atmosphere is stable; the opposite occurs in the other case.

An important point, so far not considered in stability problems, is that during the stellar evolution the star always adapts in a stabilizing way to the new values of the accelerations, in such a way that the net acceleration always remains negative. This is described by Nieuwenhuijzen and De Jager (l.c.). A consequence is that questions related to stellar atmospheric stability can not be discussed on the basis of considerations on the 'constant' accelerations but that the time dependent ones have to be taken into account. By considering the influence of the gravity

waves which, during part of their cycle, cause an outward acceleration, and by assuming that the star can be considered unstable when at any time at least one-third of the stellar surface has an outward acceleration, Fig. 9 was derived. It shows two regions of instability: the upper one is valid for redward evolving stars, the lower applies to blueward evolving ones, which are less massive than redward going ones, because they have lost a substantial part of their mass during evolution. As a consequence they are more unstable than redward evolving stars with the same luminosity and effective temperature. The lower instability region has a remarkable position and must be considered as an 'evolutionary void': stellar atmospheres should not be able to persist in that area. In this diagram the open circles are stars that were designed hypergiant on the basis of inspection of their spectra. It may be significant that the greater part of them are situated at the low-temperature side of the 'evolutionary void', and that their rate of mass loss is 3 to 10 times larger than the value that would appear from a smooth interpolation formula such as the one established by De Jager, Nieuwenhuijzen and Van der Hucht (1988). These are clear indications of

their unstable character, and these effects may explain the peculiar position of the yellow hypergiants in the HR diagram.

#### REFERENCES

- Boer, B., De Jager, C. and Nieuwenhuijzen, H.: A&A 195, 218  
Burki, G.: 1978, A&A 65, 357  
De Jager, C., De koter, A., Carpay, J., and Nieuwenhuijzen, H.: 1991, A&A 244, 131  
De Jager, C., Nieuwenhuijzen, H. and Van der Hucht, K.A.: 1988, A&A Suppl. 72, 259  
De Jager, C. and Vermue, J.: 1979, *Astrophys. Space Sci.* 62, 245  
Durrant, C.J.: 1979, A&A 73, 137  
Hearn, A.G.: 1974, A&A 31, 415  
Hines, C.O.: 1960, *Can. J. Phys.* 38, 1441

#### AUTHOR'S ADDRESS

Laboratory for Space Research  
Sorbonnelaan 2  
3584 CA UTRECHT  
The Netherlands